Electrochemical characterization of sulfur with low depth of charge/discharge in lithium sulfur batteries

CrossMark

Zhigao Yang, Shengping Wang*, Kang Dong, Yu Dai, Xinrong Lei

Faculty of Materials Science and Chemistry, China University of Geosciences, Wuhan 430074, China

ABSTRACT

In this research, a narrow charge/discharge electrochemical window is enforced for lithium sulfur batteries. In this way, the active material of the electrode (which is sulfur in the initial state) is limited to Li_2S_8 and Li_2S_3, leading the electrochemical reactions to take place in the liquid phase and thereby improving the capacity performance and cycling performance. After 50 cycles at a current density of $0.1\,mA\,cm^{-2}$, the specific capacity obtained using a narrow electrochemical window (1.95-2.45 V) ($490\,mAh\,g^{-1}$) was greater than that obtained using a wide electrochemical window (1.7-2.8 V) ($435\,mAh\,g^{-1}$). This finding demonstrates the feasibility of improving the electrochemical performance by employing a suitable electrochemical window to restrain the phase transformation to the middle liquid phase.

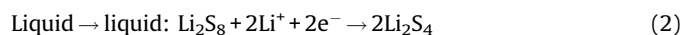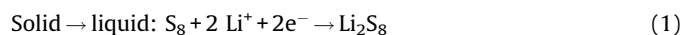© 2015 Elsevier Ltd. All rights reserved.

1. Introduction

Due to their high theoretical energy density ($2600\,Wh\,kg^{-1}$), low cost and environmental friendliness, lithium sulfur batteries are currently considered one of the most interesting battery types for future mobile and stationary applications [1–3]. However, the Li-S batteries available today lack the capacity performance and life cycle criteria needed for a broad market introduction.

Generally, lithium metal is employed as the anode material for Li-S batteries. In the charge/discharge reactions, the lithium possesses a stable electrode potential and rarely undergoes polarization. The utilization of lithium can reach almost 100% if there is excess active material in the cathode. Thus, the main hurdles to further commercialization for Li-S batteries are associated with the cathode. One such hurdle is the high solubility of the intermediate polysulfides (i.e., Li_2S_x, x = 8, 6, 4, and 3) in the electrolyte, which can shuttle between the anode and cathode, resulting in low coulombic efficiency and rapid capacity fading. Another crucial issue is the large volume expansion (~80%) of sulfur and the deposition of Li_2S_2 and Li_2S on the electrodes, which will lead to the cracking or disintegration of electrodes and degradation of the overall cell performance. However, the most pivotal challenge to the commercialization of these batteries is the highly electrically insulating nature of sulfur and Li_2S [4–7].

Various approaches for forming sulfur composites with favorable structures have been developed to address these issues. Most studies have focused on designing sulfur/carbon composites using numerous carbon matrices (e.g., ordered mesoporous carbon [8–10], carbon nanotubes/nanofibers [11–13], hollow carbon spheres [14,15], hierarchical porous carbon and graphene [16–19]) and conducting polymers, forming core-shell structures [20] or other effective packing forms [21–23] to efficiently confine sulfur in the composites and thus improve the electrochemical performance of the sulfur electrode. However, the preparation of these artful structures is usually complex and inflexible, and the limited sulfur loading allowed by the structure reduces the practical energy density. In this research, the electrochemical performances of Li-S batteries are optimized from a novel perspective: limiting the reactions to a narrow electrochemical window to achieve a high, stable specific capacity.

First, the reaction mechanism of sulfur in Li-S batteries should be analyzed. The first discharge process (theoretical capacity: $419\,mAh\,g^{-1}$) is as follows:

$$\text{Solid} \rightarrow \text{liquid: } S_8 + 2\,Li^+ + 2e^- \rightarrow Li_2S_8 \tag{1}$$

$$\text{Liquid} \rightarrow \text{liquid: } Li_2S_8 + 2Li^+ + 2e^- \rightarrow 2Li_2S_4 \tag{2}$$

The second discharge process (theoretical capacity: $1256\,mAh\,g^{-1}$) is as follows:

$$\text{Liquid} \rightarrow \text{solid: } Li_2S_4 + (2x\text{-}2)\,Li^+ + (2x\text{-}2)\,e^- \rightarrow x\,Li_2S \tag{3}$$
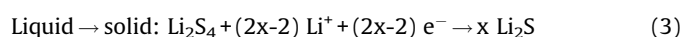
* Corresponding author.
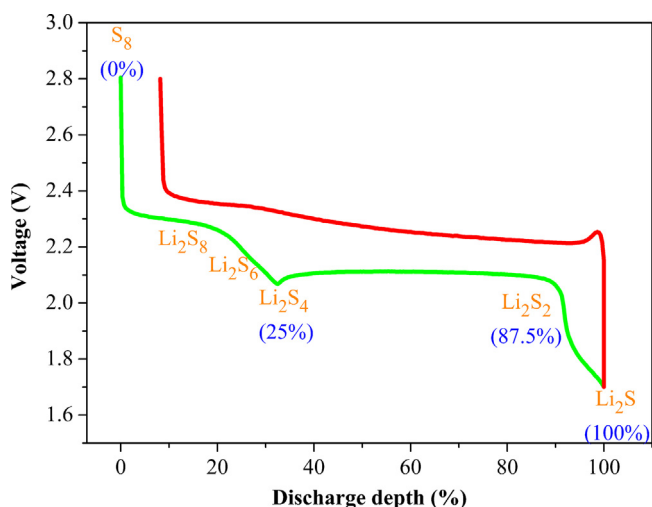 E-mail address: spwang@cug.edu.cn (S. Wang).

Fig. 1. Schematic of the repetitive phase change during the charge and discharge processes of the sulfur electrode.

As shown by Eqs. (1)–(3) and Fig. 1, the sulfur electrode undergoes a repetitive phase change [24–26] (solid-liquid-solid) during the charge and discharge process. The active materials are reduced to long-chain polysulfides (e.g., Li_2S_8), which have high solubility in the electrolyte, and then to short-chain polysulfides and finally to Li_2S/Li_2S_2. Because of its low solubility in the electrolyte, Li_2S/Li_2S_2 deposits on the conductive agent and the electrode surface. The charge reaction of the sulfur electrode is the reverse of this process.

The repetitive phase change between solid and liquid phase causes a dramatic volume change ($\sim$80%), leading to the deterioration of the electrode microstructure and the degradation of the overall battery performance. Thus, if we control the charge/discharge depth of the sulfur in the cathode to limit the reactions between Li_2S_8 and Li_2S_3, the electrochemical reactions of S will occur in a liquid system. Here, the electrochemical reactions of S only involve 12 electrons, not the 16 electrons involved in conventional Li-S batteries. However, the theoretical capacity of S is 1256 mAh g^{-1}, which is still quite impressive. Fortunately, the depth of charge/discharge for the sulfur in the cathode can be controlled by the voltage of the testing batteries. In the discharge period at 2.45 V, the solid sulfur ring molecules break, forming long-chain S_8 upon gaining electrons and being reduced. During the discharge process, the polysulfide chains continue to break. Some of these molecules are dissolved in the electrolyte on the surface of the electrode, where they undergo further reduction. When the voltage of the testing batteries is 1.95 V, S_n^{2-} (n = 3-4) is gradually reduced to Li_2S/Li_2S_2, which has low solubility and thus covers the active sites on the electrode surface. The electrochemical window of our Li-S batteries is controlled within 1.95-2.45 V. Although the dissolution of the polysulfide is inevitable [27], it can be adsorbed by carbons with high specific surface areas.

Based on the above points, sulfur/carbon composite materials were prepared by uniformly mixing elemental sulfur and high-specific-surface-area carbon to increase the conductivity of the electrode material. Meanwhile, a narrow electrochemical window (1.95-2.45 V) was adopted to the limit the depth of the charge and discharge reactions. This narrow window was used in an attempt to maintain the phase transition in the middle liquid phase and decrease the negative impact on the battery performance resulting from the repetitive electrode contraction and expansion.

2. Experiments

2.1. Pretreatment of carbon

KOH activation of carbon-based materials was used to increase the activation of acetylene black (AB) [28,29]. Acetylene black (4.00 g) and KOH (16.00 g) were mixed uniformly, placed in an alumina crucible under flowing argon and heated at a rate of 10 °C min^{-1} from room temperature to 800 °C. After maintaining the temperature at 800 °C for 1 h and then cooling to room temperature, the composite was washed with 0.1 M HNO$_3$ and deionized water until neutral. The activated acetylene black (AAB) was dried at 60 °C in air and 120 °C in vacuum for 24 h before use.

2.2. Synthesis of S/AAB composite materials

The sulfur/carbon composite was obtained using a two-step process consisting of solvent evaporation and thermal treatment. First, 0.8 g AAB and 1.2 g sulfur were added to 40 ml CS$_2$ under strong string until the solvent evaporated [30]. Next, the solid was heated in a tube furnace under argon atmosphere at a heating rate of 10 °C min^{-1} from 25 °C to 150 °C and then kept at this temperature for 24 h. The resulting material was then cooled and ground.

2.3. Material characterization

X-ray diffraction (XRD) patterns were obtained on a D8-FOCUS powder diffraction system operating at 40 kV and 40 mA with Cu-Kα radiation. The morphology of the composite materials was observed using an SU8010 high-resolution field emission scanning electron microscope (SEM) with energy dispersive X-ray spectroscopy (EDS) and a CM12 transmission electron microscope (TEM). Nitrogen sorption isotherms were obtained via Brunauer–Emmett–Teller (BET) measurements conducted using an ASAP 2020HD88 analyzer at 77 K. Thermogravimetric analysis (TGA) of the composites was conducted on an STA 449F instrument in a nitrogen atmosphere at a heating rate of 10 °C min^{-1} from room temperature to 600 °C.

2.4. Electrochemical testing

The cathode slurry was typically prepared by mixing 70 wt% composite material, 20 wt% AB and 10 wt% polyvinylidene fluoride (PVDF) binder in N-methyl-2-pyrrolidinone (NMP) solvent under magnetic stirring for 12 h. The slurry was cast on aluminum foil substrates before evaporating the solvent at 65 °C. The electrode film was cut into circular sheets with diameters of 15 mm and weights of 3 mg and further dried in a vacuum oven at 65 °C for 24 h before the testing cells were assembled. Subsequently, a type of Swagelok-type cell was used with the prepared film as the cathode, lithium foil as the anode and Celgard 2300 as the separator. All the cells were assembled in argon-filled glove box, and the electrolyte used was 1 M bis-(trifluoromethanesulfonyl) imide lithium (LiTFSI) and 0.1 M LiNO$_3$ in a mixed solvent of 1,2-dimethoxyethane (DME) and 1,3-dioxolane (DOL) with a volume ratio of 1:1. The electrolyte/sulfur (E/S) ratio in the cathode was approximately 26 μL mg^{-1} in each battery.

Galvanostatic cycling of the cells was conducted using a CT2001A battery cycler (Land, Wuhan) using a current density of 0.1 mA cm^{-2}. Electrochemical impedance spectroscopy (EIS) was performed on Biologic VMP-3 electrochemical workstation with an amplitude of 5 mV at an applied frequency range of 100 kHz to 10 MHz. The obtained impedance data were analyzed using EC-Lab V10.37 software. All experiments were conducted at room temperature.